Loss of the Calmodulin-Dependent Inhibition of the RyR1 Calcium Release Channel upon Oxidation of Methionines in Calmodulin†

Curt B. Boschek, Terry E. Jones,‡ Heather S. Smallwood, Thomas C. Squier, and Diana J. Bigelow*

Cell Biology and Biochemistry Group, Biological Sciences Division, Pacific Northwest National Laboratory, Richland, Washington 99352

Received July 9, 2007; Revised Manuscript Received November 5, 2007

ABSTRACT: The oxidation of methionines in calmodulin (CaM) can affect the activity of calcium pumps and channels to modulate the amplitude and duration of calcium signals. We have therefore investigated the possible oxidation of CaM in skeletal muscle and its effect on the CaM-dependent regulation of the RyR1 calcium release channel. Taking advantage of characteristic reductions in electrophoretic mobility determined by SDS−PAGE, we find that approximately two methionines are oxidized in CaM from skeletal muscle. The functional effect of CaM oxidation on the open probability of the RyR1 calcium release channel was assessed through measurements of [^{3}H]ryanodine binding using a heavy sarcoplasmic reticulum preparation enriched in RyR1. There is a biphasic regulation of RyR1 by unoxidized CaM, in which calcium-activated CaM acts to enhance the calcium sensitivity of channel closure, while apo-CaM functions to enhance channel activity at resting calcium levels. We find that physiological levels of CaM oxidation preferentially weaken the CaM-dependent inhibition of the RyR1 calcium release channel observed at activating micromolar levels of calcium. In contrast, the oxidation of CaM resulted in minimal functional changes in the CaM-dependent activation of RyR1 at resting nanomolar calcium levels. Oxidation does not significantly affect the high-affinity binding of calcium-activated CaM to the CaM-binding sequence of RyR1; rather, methionine oxidation disrupts interdomain interactions between the opposing domains of CaM in complex with the CaM-binding sequence of RyR1 that normally function as part of a conformational switch associated with RyR1 inhibition. These results suggest that the oxidation of CaM can contribute to observed elevations in intracellular calcium levels in response to conditions of oxidative stress observed during biological aging. We suggest that the sensitivity of RyR1 channel activity to CaM oxidation may function as part of an adaptive cellular response that enhances the duration of calcium transients to promote enhanced contractility.

Oxidatively sensitive calcium regulatory proteins that modulate the activity of calcium channels and pumps include calmodulin (CaM)[1] and phospholamban, which contain sensitive methionines whose oxidation to their corresponding methionine sulfoxides [Met(O)] results in a disruption of secondary structure that modulates the activity of the bound complex (*1*). Functionally sensitive sites of oxidation have been observed under physiological conditions, where the oxidation of an average of approximately two methionines to their corresponding methionine sulfoxides has been observed in CaM isolated from brain (*2*, *3*). Likewise, the oxidation of Met^{20} in the switch region of phospholamban has been reported to be oxidized in human heart (*4*), which will function to prevent the phosphorylation-dependent stabilization of the switch region secondary structure associated with the release of inhibition (*1*, *5*−*7*). In the case of the CaM-dependent activation of calcium pumps, the underlying mechanism of regulation has been identified; the oxidation of Met^{144} near the C-terminus of CaM prevents normal coil-to-helix structural transitions associated with CaM binding that normally disrupts the autoinhibitory interaction that keeps the pump in an inactive conformation (*1*, *8*). Likewise, the oxidation of the majority of methionines in CaM can result in a weakened CaM-dependent regulation of RyR1 and RyR2 calcium release channels, although there are currently no data regarding how lower levels of CaM

† This work was supported by NIH Grants AG12993 and AG18013. Battelle is operated for DOE under Contract DE-AC05-76RL0 1830.

* To whom correspondence should be addressed: Cell Biology and Biochemistry Group, 790 6th St., Mail Stop P7-53, Pacific Northwest National Laboratory, Richland, WA 99354. Telephone: (509) 376-2378. Fax: (509) 376-6767. E-mail: diana.bigelow@pnl.gov.

‡ Present address: Department of Physical Therapy, School of Allied Health Sciences, East Carolina University, Greenville, NC 27858.

[1] Abbreviations: β-ME, 2-mercaptoethanol; CaM, calmodulin; CaM_{ox}, calmodulin containing multiple methionine sulfoxides; C28W, CaM-binding sequence of the plasma membrane Ca-ATPase corresponding to residues L^{1100}RRGQILWFRGLNRIQTQIRVVNAFRSS^{1127}; EGTA, glycol bis(2-aminoethyl ether)-*N*,*N*,*N*′,*N*′-tetraacetic acid; DTT, dithiothreitol; HEPES, *N*-(2-hydroxyethyl)piperazine-*N*′-2-ethanesulfonic acid; HSR, heavy sarcoplasmic reticulum; IPTG, β-D-1-thiogalactopyranoside; M13, CaM-binding sequence of skeletal myosin light chain kinase corresponding to residues K^{577}RRWKKNFIAVSAANRFKKISSSGAL^{602}; Met(O), methionine sulfoxide; MS, mass spectrometry; Py, pyrene; Py_N-CaM, *N*-(1-pyrene) maleimide-labeled T34C-CaM; Py_C-CaM, *N*-(1-pyrene) maleimide-labeled T110C-CaM; Py_2-CaM, T34C/T110C-CaM labeled at both introduced cysteines with *N*-(1-pyrene) maleimide; RyRp, CaM-binding sequence of RyR1 corresponding to residues K^{3614}-SKKAVWHKLLSKQRRRAVVACFRMTPLYN ^{3643}; SDS−PAGE, sodium dodecyl sulfate−polyacrylamide gel electrophoresis; TCEP, tris-(carboxyethyl)phosphine.

10.1021/bi701352w CCC: $40.75
Published on Web 12/13/2007

oxidation, observed in tissues, regulate RyR channel function (*9*, *10*).

The ryanodine receptor (RyR) is a large (565 kDa per subunit) tetrameric calcium channel of the endo-/sarcoplasmic reticulum which mediates the release of calcium that initiates calcium-mediated processes in numerous tissues, including contraction in muscle. CaM associates with the RyR channel isoforms expressed in skeletal and cardiac muscle and in the brain (RyR1, RyR2, and RyR3, respectively) irrespective of cytosolic calcium levels and functions as a major regulatory protein in providing a sensitive modulation in response to cytosolic calcium levels (*11*, *12*). In the case of the well-studied RyR1 of skeletal muscle, binding studies using ^{35}S-labeled CaM have indicated a stoichiometry of four CaM molecules per RyR tetramer, i.e., one per subunit (*13*, *14*). Cryo-EM images have confirmed this stoichiometry showing four electron densities attributed to CaM molecules, each associated with an individual subunit of the RyR tetramer (*15*). CaM exhibits a biphasic regulation of RyR1 so that at nanomolar calcium concentrations CaM binding enhances channel activity, whereas at micromolar calcium concentrations calcium-activated CaM inhibits release of calcium by the RyR (*12*, *16*−*18*). This type of regulation, common to several other channels (e.g., the IP3 receptor, L-type calcium channels, and store-operated channels), provides a means of facilitating both rapid release and closure of channels as the initial released calcium ions bind to pre-associated CaM, converting it to the calcium-activated inhibitory species (*12*, *19*−*26*). Recent studies have indicated that apo- and calcium-activated CaM bind to distinct but overlapping regions within the primary sequence of the RyR; the amino acid sequence K^{3614}−N^{3643} (RyRp) has been identified as the high-affinity CaM binding region (*14*, *27*), while the lower-affinity CaM-binding sequence S^{1975}−R^{1999} may participate in modulation of CaM-dependent channel activity (*28*).

To examine whether the oxidation of CaM modulates the activity of RyR1 calcium release channels, we have assessed the extent of CaM oxidation in skeletal muscle and measured the relationships between the extent of CaM oxidation and both CaM-dependent increases in the open probability of the channel at resting nanomolar calcium concentrations and the CaM-dependent inhibition of channel activity at elevatated micromolar calcium concentrations. The underlying mechanisms associated with losses in RyR1 function upon CaM oxidation were identified through measurements of the binding affinity between CaM and the CaM-binding sequence of RyR1 (i.e., RyRp), which were assessed through changes in the fluorescence of Trp^{3620}. Complementary measurements of the conformation of CaM in complex with RyRp involved the covalent attachment of *N*-(1-pyrene) maleimide at engineered sites on both the N- and C-domains of CaM, permitting the assessment of contact interactions between the opposing domains of CaM in complex with the CaM-binding sequence of RyR1. We find that physiological levels of CaM oxidation selectively disrupt normal interdomain interactions for CaM in complex with RyR1 to diminish the extent of channel inhibition observed at activating micromolar calcium concentrations with a minimal effect on the ability of CaM to activate channel activity at nanomolar calcium concentrations.

EXPERIMENTAL PROCEDURES

Materials. Fischer 344 rats were purchased from the Harlan Industries (Indianapolis, IN). [^{3}H]Ryanodine was obtained from New England Nuclear (Boston, MA). HPLC-purified peptides (>95% pure) corresponding to the CaM-binding sequence of RyR1 (K^{3614}SKKAVWHKLLSKQRRRAVVACFRMTPLYN^{3643} or RyRp), the plasma membrane Ca-ATPase (L^{1100}RRGQILWFRGLNRIQTQIRVVNAFRSS^{1127} or C28W), and skeletal myosin light chain kinase (K^{577}RRWKKNFIAVSAANRFKKISSSGAL^{602} or M13) were obtained from either SynPep (Dublin, CA) or Anaspec Labs (San Jose, CA).

Escherichia coli BL21(DE3)-containing plasmids for CaM mutants containing either single cysteines in the N-domain (i.e., T34C) or C-domain (i.e., T110C) or two cysteines (i.e., T34C/T110C) were provided by R. Bieber-Urbauer (University of Georgia, Athens, GA), and following induction with β-D-1-thiogalactopyranoside, the expressed CaM was purified, essentially as previously described (*29*−*31*). All other chemicals were the purest grade commercially available.

Muscle Homogenates. Whole muscle homogenates were prepared from hind limb skeletal muscle from 6-month-old male Fischer strain 344 rats. Isolated muscles (6 g) were homogenized in a Waring blender in 18 mL of buffer A [50 mM HEPES (pH 7.5), 1 mM EDTA, and 1 mM phenylmethanesulfonyl fluoride (PMSF)] prior to centrifugation at 3000*g* for 20 min at 4 °C to remove cellular debris. The resulting pellets were resuspended in buffer A and centrifuged at 3000*g* for 20 min at 4 °C. All supernatants were combined, and these homogenates were strained through six layers of cheese cloth prior to immunoblotting. Protein concentrations were determined using the bicinchoninic acid (BCA) assay (Pierce, Rockford, IL).

SDS−*PAGE and Immunoblotting.* A 15% SDS−PAGE gel was loaded with 60 μg of cellular protein or 0.2 μg of authentic CaM standard. Proteins were electrophoretically separated at 200 V and transferred to nitrocellulose using a semidry transfer system (Bio-Rad) for 30 min at 15 V. CaM was detected with rabbit polyclonal anti-calmodulin primary antibodies (Signal Transduction Products, San Clemente, CA) and anti-rabbit secondary antibodies conjugated with horseradish peroxidase for detection with ECL Plus (Amersham Biosciences, Piscataway, NJ).

Isolation of HSR. Heavy SR vesicles corresponding to terminal cisternae of SR were prepared from F344BN hybrid rat hind limb muscles through a series of differential centrifugations, essentially as described previously (*11*, *32*). Flash-frozen muscle was thawed and homogenized at 5 mL/g in 5 mM Tris maleate (pH 6.8) and 0.1 M NaCl prior to centrifugation at 3300*g* for 30 min. Supernatants were then filtered through cheese cloth and centrifuged at 16300*g* for 30 min. Resulting pellets were resuspended in 5 mM Tris maleate (pH 6.8), 0.3 M sucrose, 0.4 M KCl, and 20 μM $CaCl_2$, subjected to a discontinuous sucrose density gradient of 22, 35, and 45% (w/v), and centrifuged at 112400*g* for 5 h. The HSR fraction at the 35%−45% interface was collected, diluted 4-fold in 10% (w/v) sucrose and 5 mM Tris maleate (pH 6.8), and centrifuged at 180000*g* for 40 min. The resulting pellets were resuspended in a minimal volume of 10% (w/v) sucrose and 5 mM Tris maleate (pH

6.8) and stored at −80 °C. All solutions contained a protease inhibitor cocktail [0.1 mM phenylmethanesulfonyl fluoride (PMSF) and aprotinin, benzamidine, leupeptin, and pepstatin (1 μg/mL each)].

[^{3}H]Ryanodine Binding. Calcium concentration dependencies of binding of [^{3}H]ryanodine to HSR vesicles were assessed essentially as previously described (*33*). Briefly, HSR vesicles (120 μg/mL) were incubated with [^{3}H]-ryanodine (20 nM) in the presence and absence of 10 μM unlabeled ryanodine (to define nonspecific binding of [^{3}H]-ryanodine) for 16−18 h at room temperature in incubation buffer [50 mM MOPS (pH 7.4), 300 mM NaCl, 100 μg/mL BSA, 0.1% CHAPS, 0.7 mM EGTA, and sufficient $CaCl_2$ to yield the desired free calcium concentration]. Free calcium concentrations were measured using ratiometric calcium sensitive dyes Fura-2, Fura-4, and Fura-6, as previously described (*34*, *35*). Free ryanodine was separated by filtration through Whatman GF/F glass fiber filters, and filters were washed five times (3 mL each) using the incubation buffer. The amount of [^{3}H]ryanodine bound to RyR1 was measured following agitation for 1 h in 5 mL of ReadyPro+ scintillation fluid (Beckman, Fullerton, CA), and radioactivity was measured using a Packard TriCarb 2100TR apparatus (Packard, Downers Grove, IL). Specific binding of [^{3}H]ryanodine to RyR1 was calculated by subtracting nonspecific binding from total binding.

Oxidation of CaM. Methionines in CaM were specifically oxidized by incubating 60 μM CaM (1 mg/mL) in 50 mM HOMOPIPES (pH 5.0), 0.1 M $MgCl_2$, and 50 mM H_2O_2 at 25 °C for variable amounts of time between 1 and 20 h, essentially as previously described (*2*). H_2O_2 concentrations were determined by using its extinction coefficient [$\epsilon_{240} = 39.4 \pm 0.2$ M^{-1} cm^{-1} (*36*)]. The oxidation reaction was terminated by dialysis at 4 °C against multiple changes of 5 mM ammonium bicarbonate (pH 7.7) and verified by gel electrophoresis or intact protein mass spectrometry. This experimental protocol for oxidizing CaM results in the exclusive oxidation of methionines to methionine sulfoxide, as determined previously by amino acid analysis (*37*).

Mass Spectrometric Analysis of Oxidized CaM. Electrospray ionization mass spectrometry (ESI-MS) was used to quantitate the distribution of CaM oxiforms and determine the average methionine sulfoxide concentration for each sample. Quantitation of the average methionine sulfoxide content was associated with a 7% error, as determined previously (*37*, *38*).

Covalent Labeling of CaM with Pyrene. CaM was specifically labeled with pyrene in either domain as previously described (*34*). Briefly, CaM mutants (T34C-CaM or T110C-CaM) in 10 mM HEPES (pH 7.8) were reduced with 0.25 μM tris(carboxyethyl)phosphine (TCEP), and then a 20-fold molar excess of *N*-(1-pyrene) maleimide was added. After incubation for 2 h, excess dye was removed with a Sephadex G25 column. The stoichiometry of bound pyrene was measured using the extinction coefficient [$\epsilon_{340} = 40\,000$ M^{-1} cm^{-1} (*39*)].

Fluorescence Emission Spectra. Spectra were acquired at 25 °C using a FluoroLog2 Spex instrument at 1 nm resolution with both excitation and emission slits set at 5 nm with an integration time of 0.1 s for spectra. Measurements of tryptophan fluorescence involved constant amounts of CaM binding peptides RyRp, M13, and C28W (1.1 μM) excited at 295 nm. Measurements of pyrene fluorescence involved constant amounts of Py-CaM (100 nM) excited at 330 nm with fluorescence emission measured at 375 nm. In all cases, measurements were taken in 50 mM MOPS (pH 7.0), 0.1 M KCl, 1 mM $MgCl_2$, 1 mM EGTA, and sufficient calcium chloride standard to yield the desired free calcium levels that were initially estimated using MaxChelator and subsequently verified using ratiometric calcium sensitive dyes Fura-2, Fura-4, and Fura-6, as previously described (*34*, *35*).

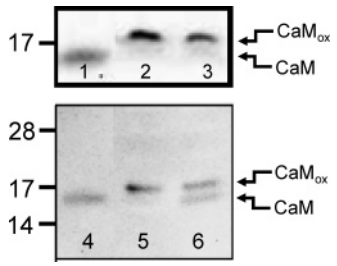

FIGURE 1: CaM oxidation in skeletal muscle. Immunoblots probed with antibodies against CaM following SDS−PAGE for an unoxidized CaM standard (expressed and purified from *E. coli*, as described in Experimental Procedures) (lanes 1 and 4), muscle homogenates from fast twitch skeletal muscle of 5-month-old (young adult) and 26-month-old (senescent) Fisher 344 rats (lanes 2 and 3, respectively; top panel), or muscle homogenates from New Zealand white rabbit (lanes 5 and 6; bottom panel). The muscle sample in lane 6 also contained unoxidized CaM added prior to sample application to the electrophoresis gel, as an internal control for any lane-to-lane variability in migration. Arrows on the right of the panel indicate positions of authentic standards of expressed and purified CaM that is unoxidized (CaM) or oxidized to a level of 2.5 methionine sulfoxides per CaM (CaM_{ox}). Protein loads are 10 μg of homogenate and/or 25 ng of purified CaM.

Fluorescence Anisotropy. Anisotropy was measured at 25 °C using a FluoroLog2 Spex instrument with both excitation and emission slits set at 5 nm with an integration time of 3 s (*40*, *41*). All measurements of tryptophan fluorescence involved constant amounts of RyRp (1.1 μM) in 50 mM MOPS (pH 7.0), 0.1 M KCl, 1 mM $MgCl_2$, 1 mM EGTA, and sufficient calcium chloride standard to yield the desired free calcium levels. Excitation was at 295 nm with fluorescence emission collected at 350 nm.

RESULTS

Oxidation of CaM in Skeletal Muscle. Immunoblots against CaM indicate a reduced electrophoretic mobility of cellular CaM in comparison to authentic controls following separation of cellular proteins in muscle homogenates by SDS−PAGE, irrespective of whether skeletal muscles were obtained from young adult or senescent Fischer 344 rats or New Zealand white rabbits (Figure 1). The decrease in electrophoretic mobility corresponding to an apparent shift of 1−2 kDa in molecular mass is indicative of the oxidation of an average of two methionines per CaM, based on electrophoretic shifts previously resolved for individual purified oxiforms of CaM (*42*). This extent of CaM oxidation is similar to that observed in CaM isolated from brains of senescent Fischer 344 rats (*2*, *42*). We note that other commonly observed post-translational modifications (e.g., acetylation, methylation, and nitration) do not result in these characteristic mobility shifts (*2*, *43*). In contrast to the presence of oxidized CaM in young as well as senescent muscle, CaM is known to remain unoxidized in the young brain, with progressive increases

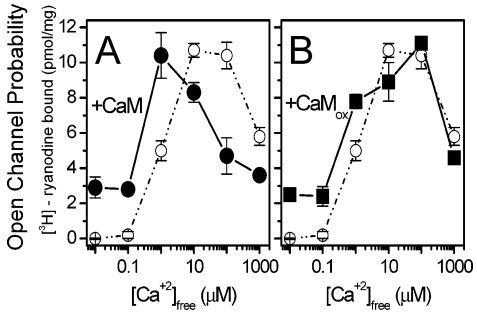

FIGURE 2: Oxidation of methionines in CaM results in the selective loss of the CaM-dependent inhibition of RyR1. Calcium-dependent regulation of RyR1 channel open probability measured using binding of [^{3}H]ryanodine to a heavy SR preparation (120 μg/mL) in the absence (○) and presence of wild-type (●) (A) or mildly oxidized (■) (B) CaM (250 nM). Mildly oxidized CaM contains an average of approximately two Met(O) per CaM. Ryanodine binding was assayed in 50 mM MOPS (pH 7.4), 300 mM NaCl, 100 μg/mL albumin, 0.1% CHAPS, 20 nM [^{3}H]ryanodine, 0.7 mM EGTA, and sufficient $CaCl_2$ for the indicated free calcium concentrations as described in Experimental Procedures. Average values and standard errors are shown from measurements using three different preparations.

in the extent of Met oxidation during aging (*2*). These results indicate a tissue-dependent sensitivity of protein oxidation and are consistent with the substantially larger amount of oxidation in muscle as compared with brain (*44*). The observation that in vivo CaM oxidation is limited to an average of two (of nine) Mets per CaM is consistent with the observed preferential degradation of more highly oxidized CaM by the proteasome−Hsp90 complex, correlating with tertiary structural changes induced by the oxidation of selected methionines (i.e., Met^{145}) (*42*, *45*). Further, prior measurements have demonstrated a diminished activation of some target proteins (e.g., the plasma membrane Ca-ATPase) upon the selective oxidation of individual methionines (i.e., Met^{144}), indicating that the retention of two methionine sulfoxides in CaM has the potential to affect the activity of CaM-dependent enzymes. To assess the possible functional effects of CaM oxidation on rates of calcium release in muscle, we have examined the effect of methionine oxidation in CaM on the regulation of the RyR1 calcium release channel, whose kinetics of activation and inhibition contribute to the magnitude and duration of the calcium transient associated with excitation−contraction coupling.

Oxidation of CaM Results in Selective Loss of the CaM-Dependent Inhibition of RyR1. To determine the functional effect of methionine oxidation in CaM on the biphasic regulation of RyR1, alterations in the calcium dependence of [^{3}H]ryanodine binding were measured to assess channel function in the presence of oxidized CaM in comparison with that of native CaM (Figure 2). Ryanodine preferentially binds to the open state of the RyR tetramer, providing a specific steady state measure of channel open probability (*46*). These measurements used a heavy SR fraction isolated from rat hind limb skeletal muscle, which is enriched in RyR1 and lacks endogenously bound CaM (*32*). Magnesium was excluded from these functional assays of RyR1, i.e., [^{3}H]-ryanodine binding, since Mg^{2+} is an inhibitor of channel activity and reduces the overall magnitude of the signal needed for a quantitative determination of the effects of CaM oxidation on RyR1 function (*47*). Functional measurements of the effect of CaM oxidation on RyR1 function were made following the in vitro oxidation of approximately two Mets to their corresponding methionine sulfoxides (MetSO) using hydrogen peroxide, resulting in an average extent and pattern of oxidation that are similar to those observed in vivo (Table 1) (*2*, *48*).

At low calcium levels, associated with resting muscle (i.e., <0.1 μM free calcium), [^{3}H]ryanodine does not bind to RyR1, indicating that the channel is closed. A progressive increase in the fraction of open channels upon increasing the free calcium concentration is observed, with maximal [^{3}H]ryanodine binding (i.e., 11 pmol/mg) between 10 and 100 μM free calcium. At higher calcium concentrations, the level of [^{3}H]ryanodine binding is decreased, consistent with prior observations indicating an endogenous calcium-dependent regulation of the RyR1 channel isolated from rabbit muscle (*12*, *49*, *50*). Addition of saturating amounts of CaM (i.e., 250 nM) increases the fraction of open channels at resting calcium levels and shifts the calcium dependence of channel opening to lower calcium concentrations, with maximal [^{3}H]ryanodine binding occurring at approximately 1 μM free calcium, essentially as previously reported (*12*). Further, the calcium dependence of channel inactivation is shifted by 2 orders of magnitude toward lower calcium levels. Thus, CaM association functions to adjust the inherent calcium sensitivity of RyR1 channel open probability, serving as an activator at nanomolar free calcium concentrations and an inhibitor at higher micromolar calcium levels.

In comparison to unoxidized CaM, addition of oxidized CaM to heavy SR modulates the calcium sensitivity of channel activity at micromolar calcium concentrations (Figure 2B). Thus, at nanomolar calcium concentrations, an extent of channel activation similar to that of unoxidized CaM is observed. In contrast, at higher micromolar calcium concentrations, the normal CaM-dependent inhibition of channel activity is substantially diminished upon oxidation of two methionines in CaM. These differences in [^{3}H]-ryanodine binding are most salient as evidenced by the shift in the peaks of binding curves from 1 μM free calcium, in the presence of CaM (Figure 2A), to 100 μM free calcium, in the presence of oxidized CaM (Figure 2B). These results suggest that physiologically observed levels of CaM oxidation will result in a diminished extent of channel closing in vivo.

The sensitivity of RyR1 channel activity to the extent of CaM oxidation was further explored using CaM samples with variable levels of methionine oxidation, which were quantitatively determined using intact protein mass spectrometry. Using these oxidation conditions, Mets were exclusively oxidized (*31*), and the most extensively oxidized CaM species (i.e., 16 850 Da) corresponded to the theoretical mass of CaM plus nine oxygens (i.e., 16 706 Da + 144 Da = 16 850 Da) (Table 1). At nanomolar calcium concentrations, the CaM-dependent activation of RyR1 channel activity is relatively insensitive to the extent of CaM oxidation; a significant loss of RyR1 channel activation is only observed at higher levels of methionine oxidation (i.e., >4 MetSO/CaM), where 50% inhibition requires the oxidation of 6 MetSO/CaM (Figure 3A). In contrast, the CaM-dependent inhibition of channel activity, observed at micromolar calcium levels associated with muscle activation, is highly sensitive to modest levels of methionine oxidation in CaM. The half-point associated with the loss of CaM-dependent inhibition of channel activity

Table 1: Oxiform Distribution in Oxidized CaM Measured by ESI-MS[a]

no. of MetSO/CaM	theoretical mass (Da)	experimental mass (Da)	fractional contribution					
0	16 706	16 707 ± 2	1.0	0.09	0	0	0	0
1	16 722	16 724 ± 2	0	0.21	0.10	0.02	0	0
2	16 738	16 741 ± 1	0	0.29	0.15	0.05	0	0
3	16 754	16 758 ± 3	0	0.17	0.21	0.10	0.02	0
4	16 770	16 771 ± 2	0	0.07	0.18	0.17	0.03	0
5	16 786	16 788 ± 2	0	0.09	0.10	0.19	0.11	0
6	16 802	16 804 ± 2	0	0.08	0.08	0.12	0.19	0.16
7	16 818	16 819 ± 1	0	0	0.08	0.13	0.19	0.14
8	16 834	16 834 ± 3	0	0	0.06	0.10	0.23	0.12
9	16 850	16 852 ± 2	0	0	0.04	0.12	0.23	0.58
average MetSO/CaM			0	2.5	4.1	5.6	7.1	8.1

[a] Relative contributions of different oxiforms of CaM (MetSO/CaM) determined from deconvolution of intact protein ESI-MS spectra, essentially as previously described (*2*, *37*), where experimental masses represent the averages and standard deviations for more than three different samples. Different extents of methionine oxidation were the result of varying exposure times for CaM (60 μM) in 50 mM HOMOPIPES (pH 5.0), 0.1 M $MgCl_2$, and 50 mM H_2O_2 at 25 °C.

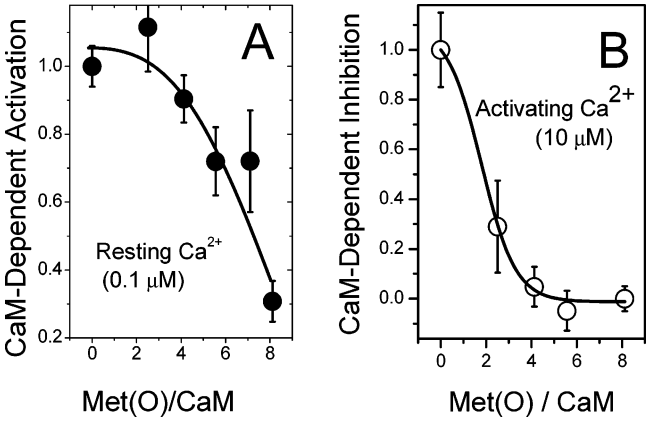

FIGURE 3: Loss of CaM-dependent regulation of RyR1 upon oxidation of Mets in CaM. CaM-dependent activation (A) and inhibition (B) of RyR1 measured at resting (0.1 μM) (A) and activating (10 μM) (B) calcium concentrations as a function of the average number of methionines oxidized to their corresponding methionine sulfoxides, which was determined by mass spectrometry (Table 1). CaM-dependent regulation of RyR1 was assessed as the absolute value of differences in [^{3}H]ryanodine binding in the presence and absence of added CaM. Average extents of CaM oxidation, expressed as the molar ratio of Met(O) to CaM, were determined by ESI-MS as described in Experimental Procedures. Assay conditions are as described in the legend of Figure 2. Average values and standard errors are shown from measurements using three independent determinations.

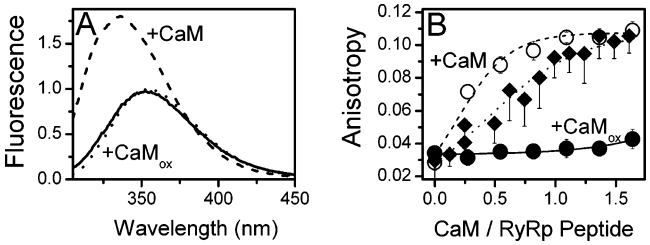

FIGURE 4: Disruption of binding between apo-CaM and RyRp upon oxidation of Mets in CaM. Fluorescence emission spectra (A) and anisotropy (B) of the Trp anchor residue in the CaM-binding sequence of RyR1 (i.e., RyRp). Spectra in panel A are shown for 1.1 μM RyRp alone (•••) or following addition of either unoxidized CaM (- - -) or CaM_{ox}, where CaM is extensively oxidized with an average oxidation state of 8.1 Met(O) per CaM (—). Anisotropy values in panel B are shown for RyRp in the presence of unoxidized CaM (- - -○- - -) or in the presence of oxidized CaM, where CaM is oxidized at physiological levels, i.e., with an average oxidation state of 2.5 Met(O) per CaM as described in Table 1 (•••, ◆; non-symmetrical error bars are shown for clarity), or extensively oxidized CaM (—●—). Fluorescence emission spectra were acquired in the presence of 1.7 μM CaM. λ_{ex} = 295 nm, and λ_{em} = 350 nm (B). Buffer included 50 mM MOPS (pH 7.0), 0.1 M KCl, 1 mM $MgCl_2$, and 1 mM EGTA (resulting in 5 nM free calcium).

corresponds to the oxidation of 2 MetSO/CaM (Figure 3B). These results indicate a functional dichotomy with respect to the modulation of RyR1 channel activity upon oxidation of methionines in CaM and suggest that physiological levels of CaM oxidation selectively modulate the CaM-dependent inhibition of channel activity to increase the extent of release of calcium from the SR. However, higher levels of CaM oxidation abolish both the CaM-dependent activation and inhibition of channel activity.

Oxidation of Mets in Apo-CaM Results in Weakened Binding to RyR1. The C-terminal domain of apo-CaM selectively associates with the N-terminal region in the CaM-binding sequence (K^{3614}—N^{3643}) of RyR1 (i.e., RyRp) which includes Trp^{3620} (*51*), permitting facile measurements of binding through changes in either the fluorescence intensity or rotational dynamics (i.e., anisotropy) of this single Trp residue. CaM itself has no Trp residues in its sequence, making the intrinsic fluorescence of Trp^{3620} a unique signal. Upon association of unoxidized apo-CaM with RyRp, there is a 1.8-fold increase in fluorescence intensity and a 20 nm blue shift in the emission spectrum of Trp^{3620} of RyRp (Figure 4A). Likewise, a progressive increase in Trp anisotropy is observed upon association of apo-CaM with RyRp that saturates at a molar stoichiometry of 1:1 (Figure 4B). These latter results are consistent with prior measurements by Meissner and co-workers that demonstrated a high-affinity binding interaction between apo-CaM and RyR1 (*12*). In the majority of these measurements, we have routinely included $MgCl_2$ in our measurements of binding of CaM to target peptides, since magnesium can compete with calcium to affect the kinetics of CaM binding. However, under equilibrium binding conditions, the presence of magnesium in the buffer does not affect the binding affinity of CaM for the CaM-binding sequence of RyR1, in agreement with earlier measurements for other CaM-dependent enzymes (*52*).

Following the oxidation of approximately two methionines to their corresponding methionine sulfoxides in CaM, the ability of oxidized apo-CaM to bind to the CaM-binding sequence of RyR1 is retained, albeit with a reduced binding affinity. The binding curve shows a modest shift toward

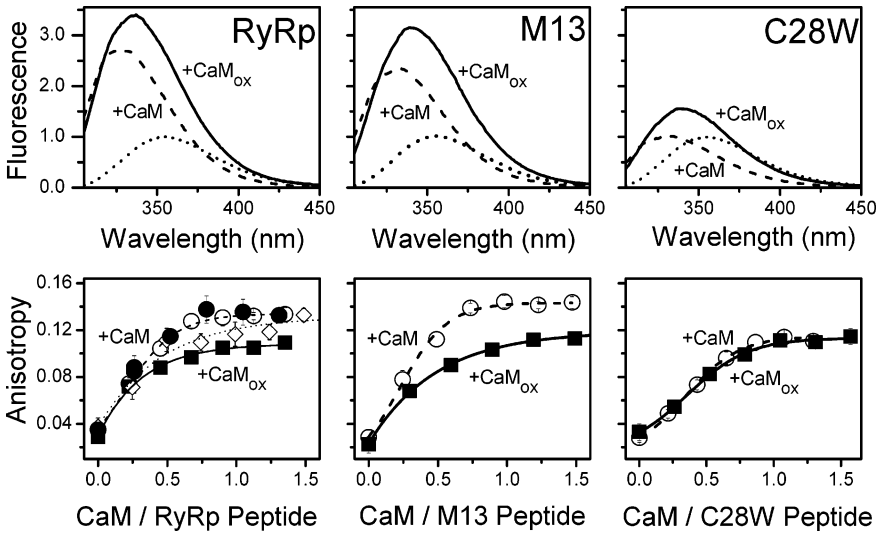

FIGURE 5: High-affinity binding between calcium-activated CaM and the RyRp is insensitive to Met oxidation in CaM. Fluorescence emission spectra (top panels) and anisotropy changes (bottom panels) of Trp anchor residues in CaM-binding sequences of RyR1 (RyRp) (left panels), myosin light chain kinase (M13) (middle panels), and the plasma membrane Ca-ATPase (C28W) (right panels) in the presence of oxidized or unoxidized CaM. Spectra are shown in each case for the indicated peptide alone (⋯) or following addition of either unoxidized CaM (- - -) or extensively oxidized CaM (—). Anisotropy plots are shown for the indicated peptide in the presence of unoxidized CaM (- - -○- - -) or oxidized CaM with an average of either 2.5 Met(O) per CaM (⋯◇⋯) or 8.1 Met(O) per CaM (—■—). In the top panels, fluorescence emission spectra were acquired in the presence of 1.7 μM CaM. λ_{ex} = 295 nm, and λ_{em} = 350 nm (bottom panels). Buffer conditions for all experiments included the relevant CaM-binding sequence at 1.1 μM, up to 1.7 μM CaM, 50 mM MOPS (pH 7.0), 0.1 M KCl, 1 mM EGTA, 1.7 mM $CaCl_2$ (700 μM free calcium), and either no $MgCl_2$ (●) or 1 mM $MgCl_2$ (○, ◇, and ■).

higher [CaM]/[RyRp] stoichiometries, with complete binding requiring ~30% more CaM. In the functional measurements using the intact receptor, this modest decrease in binding affinity is overcome by the inclusion of saturating amounts of CaM (Figure 2). On the other hand, following extensive oxidation of CaM (where the predominant oxiform has nine methionine sulfoxides per CaM; see Table 1), there is essentially no change in either Trp fluorescence intensity or anisotropy upon titration of apo-CaM with RyRp. These measurements indicate a substantial decrease in the affinity between highly oxidized CaM and RyRp at nanomolar calcium concentrations. These latter results are consistent with the nearly complete loss of RyR1 activation following the oxidation of the majority of methionines in CaM (Figure 3). Thus, the observed progressive loss of the CaM-dependent activation of RyR1, which correlates with the number of oxidized methionines in apo-CaM, is due to a diminished binding affinity. This latter conclusion agrees with earlier observations of Balog and co-workers, who reported decreases in affinity between oxidized apo-CaM and RyR1 (*9*).

Retention of High-Affinity Binding between Calcium-Activated CaM and RyR1 following Oxidation of Methionines. The structure of calcium-activated CaM in association with RyRp has been determined and is similar to that of other classical CaM-binding sequences such as M13 from skeletal myosin light chain kinase and C28W from the plasma membrane Ca-ATPase, in that the C-terminal domain of CaM associates with the hydrophobic Trp anchor in RyRp in a collapsed structure that brings its opposing domains of CaM into the proximity of each other (*51*, *53*−*55*). Further, prior results have demonstrated that structural changes in RyRp associated with the calcium-dependent binding of CaM to RyRp reflect the functional modulation of the RyR channel (*56*). Consistent with these expectations, in comparison with apo-CaM, the association of calcium-activated CaM with RyRp results in a substantially larger change in the spectral properties of Trp^{3620}; i.e., there are a 2.7-fold increase in fluorescence intensity and a 27 nm blue shift in the emission spectrum of Trp^{3620} (Figure 5). In comparison with that of unoxidized CaM, binding of oxidized CaM to all three CaM-binding sequences induces smaller (18 nm) spectral blue shifts and an increased fluorescence intensity consistent with an altered binding mechanism.

Fluorescence anisotropy measurements indicate a high-affinity binding interaction between calcium-activated CaM and the CaM-binding sequence of RyR1 (Figure 5), which are consistent with earlier measurements that indicated an apparent dissociation constant near 60 ± 10 nM (*56*). Neither physiological levels of oxidation (approximately two methinionine sulfoxides per CaM) nor the oxidation of essentially all nine methioinines in CaM to their corresponding methionine sulfoxides alters the affinity between calcium-activated CaM and the CaM-binding sequence (RyRp). Indeed, the high-affinity binding between calcium-activated CaM and the CaM-binding sequences of all three CaM-dependent proteins is retained irrespective of the oxidation of all nine methionines in CaM, as assessed by increases in Trp anisotropy that are saturated upon addition of an equimolar concentration of either unoxidized or fully oxidized CaM (Figure 5).

There is a decrease in the steady state Trp anisotropy for the bound complex between CaM and RyRp, which is dependent on the extent of CaM oxidation. Oxidation of all nine Mets in CaM results in a decrease in the maximal anisotropy for CaM bound to RyRp from 0.133 to 0.108. The decrease in anisotropy is indicative of increased mobility due to either alterations in the binding site environment associated with the Trp within RyRp or differences in the flexibility of the overall complex. This result strongly suggests that the observed loss of the CaM-dependent inhibition of the intact RyR1 upon the progressive oxidation of CaM is not due to a loss in binding affinity, but rather

due to an abnormal and nonfunctional mode of binding. In comparison to the complex with unoxidized CaM, comparable decreases in Trp anisotropy are observed for the complex between oxidized CaM and the CaM-binding sequences of RyR1 (i.e., RyRp) and myosin light chain kinase (M13). Anisotropy values for the CaM-binding sequence of the Ca-ATPase (C28W) are comparable to those for fully oxidized CaM bound to either RyRp or M13. The insensitivity of the measured Trp anisotropy in C28W to CaM oxidation may be related to the considerable flexibility that arises due to differences in the sequences of the three different CaM-binding sequences, as the presence of small amino acids near Trp^{1107} in C28W (e.g., Gly^{1110}) will destabilize the helical structure to enhance the rotational dynamics of Trp^{1107}.

Retention of Calcium-Induced Disruption of Interdomain Interactions in CaM following Met Oxidation. As high-affinity binding of calcium-activated CaM to RyRp is retained following oxidation of all nine methionines of CaM, it is apparent that the functional sensitivity of the calcium-dependent inhibition of RyR1 (Figure 3B) is related to alterations in the conformation of oxidized CaM bound to RyRp. We have, therefore, assessed calcium-dependent structural changes within the C- and N-terminal domains of CaM as well as possible changes in interdomain coupling through fluorescence measurements in which the fluorophore *N*-(1-pyrene) maleimide was covalently labeled at engineered cysteines in the N- and C-domains of CaM.

Py_N-CaM and Py_C-CaM correspond to CaM mutants with a single *N*-(1-pyrene) maleimide bound at engineered cysteines T34C and T110C, respectively, and permit an assessment of the calcium-dependent activation of the individual domains. Py_2-CaM contains two *N*-(1-pyrene) maleimide fluorophores bound at both introduced cysteines (i.e., T34C/T110C) and permits the assessment of interdomain contact interactions (*34*). We have previously demonstrated that binding to RyRp induces calcium-dependent conformational changes within N- and C-terminal globular domains of CaM that mirror the calcium dependence of CaM regulation of the intact RyR1 calcium release channel (*56*). These measurements take advantage of the sensitivity of pyrene fluorescence to small changes in the local environment and the ability of these chromophores to form excited state dimers when two fluorophores come within 10 Å of one another (*57*). Py_2-CaM exhibits excimer fluorescence (480 nm) in solution at nanomolar calcium concentrations (apo-CaM) (Figure 6A), indicating that a significant fraction of CaM conformers exhibit intramolecular interactions between N- and C-terminal domains. On the other hand, calcium binding increases the fraction of conformers associated with extended conformations, as evidenced by diminished excimer fluorescence (480 nm) with a concomitant increase in monomer fluorescence (400 nm) (*34*) (Figure 6A). Calcium-dependent changes in the local environment within N- and C-terminal globular domains are also evident from monomer fluorescence changes of pyrene labeled within each individual domain.

Upon oxidation of all nine methionines to Met(O), the spectra of apo-Py_2-CaM and calcium-activated Py_2-CaM remain very similar to that of unoxidized Py_2-CaM; i.e., a dramatic reduction in the extent of excimer formation associated with calcium activation is retained in oxidized CaM (Figure 6B). A small (i.e., 30%) reduction in the excimer fluorescence is associated with oxidized apo-CaM in comparison with unoxidized CaM, which is consistent with prior measurements indicating the disruption of tertiary structural interactions upon the oxidation of CaM (*37*, *42*, *45*, *58*). These results indicate that the oxidation of all nine methionines in CaM does not substantially affect the stabilization of the calcium-activated state associated with target protein binding.

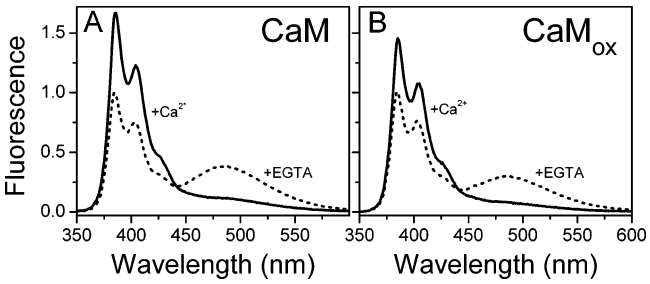

FIGURE 6: Retention of calcium-dependent structural coupling between opposing domains of oxidized CaM. Fluorescence emission spectra for unoxidized (A) or oxidized (B) apo-Py_2-CaM (- - -) and calcium-activated (—) Py_2-CaM (100 nM). Buffer included 50 mM MOPS (pH 7.0), 0.1 M KCl, 1 mM $MgCl_2$, and 1 mM EGTA in the absence or presence of 1.7 mM $CaCl_2$, resulting in free calcium concentrations of 5 nM (apo-CaM) or 700 μM (calcium-activated CaM).

Weakened Binding of Calcium to Oxidized CaM. To investigate how methionine oxidation may affect normal structural changes associated with calcium activation, we have compared the calcium dependence of conformational changes in the C- and N-domains of unoxidized and oxidized CaM, measured using Py_C- and Py_N-CaM, as well as interdomain interactions from Py_2-CaM (Figure 7 and Table 2). In all cases, the oxidation of CaM results in shifts in the calcium concentrations of fluorescence changes, requiring 2- and 3.5-fold larger calcium concentrations for N- and C-terminal domain activation, respectively. Disruption of interdomain interactions occurs upon calcium activation of the C-terminal domain irrespective of the extent of oxidation. However, in contrast to the sequential activation of the C- and N-domains of CaM that is normally observed in unoxidized CaM, the full activation of both N- and C-terminal domains in oxidized CaM occurs at approximately the same calcium concentration. The simultaneous activation of both domains in oxidized CaM has the potential to affect the binding mechanism with target proteins, as CaM normally undergoes a multistep conformational rearrangement upon association with target proteins (*59*, *60*).

Methionine Oxidation Disrupts Contact Interactions between Opposing Domains of CaM upon Association with RyRp. Upon association of calcium-activated CaM with RyR1 and many other CaM-binding sequences, the opposing domains of CaM are brought into the proximity of each other, where contact interactions between the N- and C-domains of CaM promote the formation of a stable complex that is associated with target protein activation (*51*, *55*, *61*). Using Py_2-CaM, we are able to detect the structural interactions between the N- and C-domains of CaM upon binding to the CaM-binding sequences of RyR1 (i.e., RyRp) as well as myosin light chain kinase (M13) and the Ca-ATPase (C28W) (Figure 8). The amount of excimer formation is considerably larger for Py_2-CaM in association with either M13 or C28W,

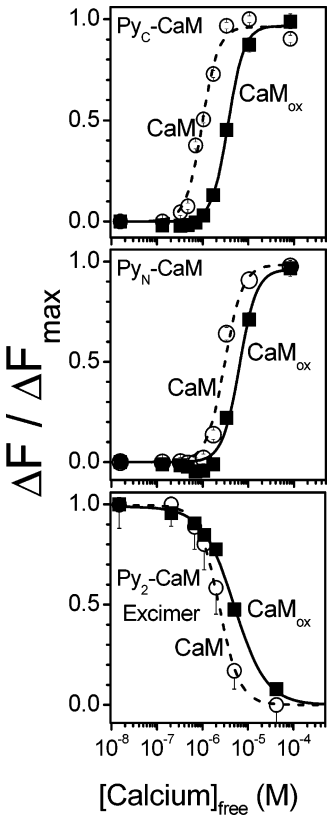

FIGURE 7: Decreased calcium affinities following CaM oxidation. Calcium dependence of fluorescence changes (i.e., $\Delta F/\Delta F_{max}$) associated with the activation of N- and C-terminal domains of unoxidized CaM (- - -○- - -) or CaM_{ox} (—■—) measured using Py_C-CaM (top panel) or Py_N-CaM (middle panel) in comparison with the disruption of interdomain interactions measured as a decrease in the level of excimer formation using Py_2-CaM (bottom panel). Experimental conditions included CaM (100 nM) in 50 mM MOPS (pH 7.0), 0.1 M KCl, 1 mM $MgCl_2$, 1 mM EGTA, and sufficient calcium chloride standard to yield the desired free calcium levels. $\lambda_{ex} = 330$ nm, and $\lambda_{em} = 375$ nm. Symbols and error bars represent three independent measurements and the associated standard errors of the mean.

Table 2: Macroscopic Dissociation Constants for Binding of Calcium to CaM[a]

	unoxidized CaM			fully oxidized CaM		
sample	$[Ca^{2+}]_{1/2}$ (μM)	K_d (μM)	n	$[Ca]_{1/2}$ (μM)	K_d (μM)	n
Py_C-CaM	1.0 ± 0.1	1.0 ± 0.1	2.5 ± 0.4	3.5 ± 0.2	3.6 ± 0.2	2.5 ± 0.2
Py_N-CaM	2.7 ± 0.1	3.0 ± 0.3	2.2 ± 0.6	5.9 ± 0.5	6.4 ± 0.6	2.3 ± 0.3
Py_2-CaM	2.1 ± 0.1	2.3 ± 0.3	1.9 ± 0.4	4.9 ± 0.4	5.0 ± 0.3	1.2 ± 0.1

[a] Calcium binding was assessed by fitting the fluorescence changes of PyC-CaM, PyN-CaM, or Py2-CaM, where calcium concentrations associated with half-maximal conformational change ($[Ca]_{1/2}$), macroscopic dissociation constants (K_d), and Hill coefficients (n) were obtained from fits of the data in Figure 7 to the Hill equation, i.e., $\Delta F/\Delta F_{max} = [Ca^{2+}]^n/(K^n + [Ca^{2+}]^n)$, are given.

than with RyRp which is consistent with the shorter distance between the binding sites for the C- and N-domains of CaM in the primary sequence of these peptides, which contain a 1−14 CaM-binding motif (*53*−*55*, *61*). In comparison, the smaller amount of excimer formation for CaM in association with RyRp is consistent with the larger separation between the binding sites for the C- and N-domains of CaM in the primary sequence of RyRp, which contains a 1−17 CaM-binding motif (*51*). In all cases, large decreases in the extent

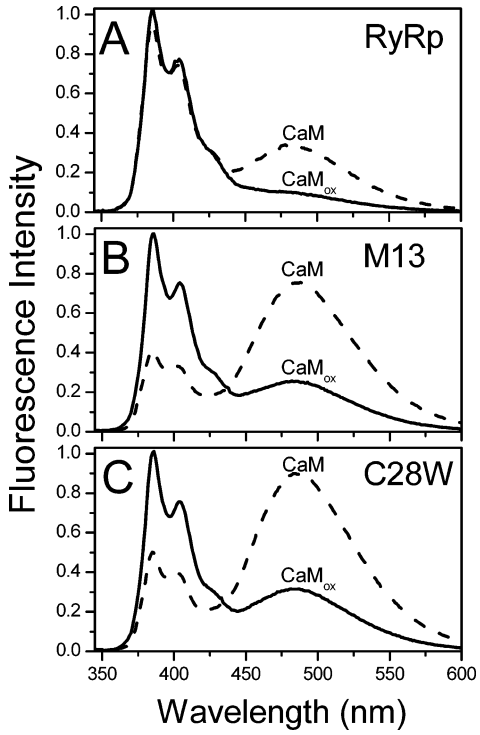

FIGURE 8: Oxidation of methionines in calcium-activated CaM disrupts interdomain interactions between opposing domains of CaM bound to RyRp. Fluorescence emission spectra of unoxidized (- - -) and oxidized (—) Py_2CaM (100 nM) in association with 120 nM of CaM-binding sequences RyRp (A), M13 (B), and C28W (C) of RyR1, MLCK, and the Ca-ATPase, respectively. Experimental conditions included 50 mM MOPS (pH 7.0), 0.1 M KCl, 1 mM $MgCl_2$, 1 mM EGTA, and 1.7 mM $CaCl_2$, yielding 700 μM free calcium. $\lambda_{ex} = 330$ nm.

of excimer formation are observed upon association of oxidized CaM with each peptide (Figure 8). The oxidation of essentially all methionines in CaM almost completely abolishes the structural coupling between the opposing domains of CaM in association with RyRp. These results, along with the binding measurements, indicate that upon oxidation of the majority of methionines to form methionine sulfoxides, calcium-activated CaM binds in an altered conformation to the CaM-binding sequence of RyR1 that does not induce the normal structural changes between subunits of the channel associated with the conformational switching necessary for channel inhibition.

DISCUSSION

Summary of Results. We have identified the oxidation of CaM in skeletal muscle, detected by characteristic reductions in electrophoretic mobility, that are indicative of the presence of approximately two methionine sulfoxides per CaM (Figure 1). This level of CaM oxidation results in the selective abolition of the normal CaM-dependent inhibition of RyR1 channel activity observed at micromolar calcium levels associated with force generation in muscle (Figures 2B and 3B). In comparison, this extent of CaM oxidation has essentially no effect on the CaM-dependent activation of RyR1 observed at resting (nanomolar) calcium levels (Figures 2B and 3A). With mild oxidation, both apo-CaM and calcium-activated CaM remain tightly associated with the CaM-binding sequence of RyR1; indeed, high-affinity binding between RyRp and the calcium-activated form of

oxidized CaM is retained following the oxidation of nearly all nine Mets (Figure 5). Similar high-affinity binding is retained between the calcium-activated form of oxidized CaM and CaM-binding sequences from both myosin light chain kinase (M13) and the plasma membrane Ca-ATPase (C28W). These results indicate that the observed disruption of normal CaM function in promoting channel closure at activating calcium levels in RyR1, and the inhibition of the Ca-ATPase by oxidized CaM, is due to alterations in the structure of the bound complexes. Indeed, CaM oxidation results in the selective disruption of the structural coupling between the opposing N- and C-terminal domains of CaM normally associated with the regulation of enzyme activities (Figure 8). Thus, it is expected that common mechanisms associated with the nonproductive association between oxidized CaM underlie the diminished functional regulation of a range of different target proteins. In the case of RyR1, the selective loss of the CaM-dependent inhibition of RyR1 at activating micromolar calcium levels will result in a longer calcium transient to enhance force generation under conditions of oxidative stress where the modification of contractile proteins adversely affects muscle tension and rates of contraction (*62*, *63*). This hypothesis is consistent with previous work demonstrating that elimination of the calcium-dependent inactivation of L-type channels results in dramatic prolongation of action potentials in cardiomyocytes (*19*).

Nonproductive Association between Oxidized CaM and RyR1. Oxidation of multiple methionines to their corresponding methionine sulfoxides has previously been observed in CaM isolated from brains of senescent Fischer 344 rats. However, as CaM is not oxidized in the brains of young animals, these results suggested a linkage between CaM oxidation and the observed age-related calcium dysfunction involving an approximate 3-fold elevation in cytosolic calcium levels (*1*, *2*, *48*). Our current results indicate the oxidation of CaM in skeletal muscle from young, disease-free animals (Figure 1). The high levels of methionine oxidation for CaM in muscle are consistent with the substantially higher levels of oxidative stress in muscle in comparison to other tissues (*44*). The appearance of mildly oxidized CaM in vivo is consistent with the previously documented preferential degradation of more highly oxidized CaM species by the proteasome−Hsp90 complex (*42*).

The oxidation of methionines in CaM is expected to affect the activities of a range of different muscle proteins and has previously been shown to disrupt the normal CaM-dependent regulation of the plasma membrane Ca-ATPase, nitric oxide synthase, CaM-dependent protein kinase II, and RyR calcium release channels (*9*, *10*, *64*−*66*). The mechanism underlying inhibition of the Ca-ATPase by oxidized CaM has been most extensively studied and arises as a result of the structural uncoupling between the opposing domains of CaM after the site-specific oxidation of Met^{144} in CaM, which essentially locks the enzyme in a less active state (*1*, *8*, *45*, *54*, *58*, *67*). In contrast, the loss of RyR functional regulation upon the oxidation of the majority of the methionines in CaM has previously been suggested to arise due to a diminished affinity between the RyR calcium channel and both apo or calcium-activated forms of oxidized CaM (*9*, *10*).

Our results confirm prior observations regarding the functional sensitivity associated with the CaM-dependent regulation of RyR1 channel function at high levels of CaM oxidation (Figures 2B and 3) (*9*) and indicate that the inability of oxidized CaM to activate the RyR1 channel at resting nanomolar calcium levels is due to weakened CaM binding (Figure 4). However, our work has addressed, for the first time, the effects of lower extents of methionine oxidation that we have shown are characteristic of that observed in skeletal muscle (Figure 1). These measurements indicate that there is little functional sensitivity in the CaM-dependent activation of RyR1 channel activity at nanomolar calcium concentrations associated with resting muscle (Figure 3A). Rather, upon oxidation of approximately two methionines to their corresponding methionine sulfoxides, as observed in CaM isolated from muscle, there is a selective disruption of the normal CaM-dependent inhibition of channel function relative to that normally observed at activating micromolar calcium levels (Figure 3B). Indeed, the high-affinity association between the calcium-activated form of CaM and the CaM-binding sequence of RyR1 is retained irrespective of the extent of Met oxidation (Figure 5), which is seen for the Ca-ATPase (C28W) and myosin light chain kinase (M13). A similar high-affinity association between the calcium-activated form of oxidized CaM and the intact Ca-ATPase mirrors that observed for the C28W peptide. In all instances, the oxidation of methionines in CaM results in an altered binding mechanism such that the interdomain contact interactions between the opposing domains of CaM normally associated with target protein binding are disrupted (Figure 8).

An understanding of the apparent disagreement between our results, which indicate a preferential disruption in the CaM-dependent activation of RyR1 at micromolar calcium concentrations (Figures 3 and 8), and those previously reported by Balog and co-workers, which suggested the preferential loss of the CaM-dependent activation of the RyR1 channel at nanomolar calcium concentrations, can be reached from a consideration of the masses for oxidized CaM used in each study (*9*). We find the selective oxidation of multiple methionines (Table 1), where the mass of the predominant oxiform of extensively oxidized CaM (i.e., 16 852 $\pm$ 2 Da) is in good agreement with the theoretical mass of CaM in which all nine methionines are oxidized to their corresponding methionine sulfoxides (i.e., 16 850 Da). In contrast, consideration of the mass spectrum for fully oxidized CaM reported by Balog and co-workers (the approximate mass of oxidized CaM was 16 880 Da) indicates either oxidation of additional sites within CaM (e.g., oxoHis) or oxidation of some methionines to their corresponding methionine sulfones ($MetSO_2$); such extensive oxidation may contribute to the observed loss of affinity between calcium-activated CaM and RyR1. Further, unlike prior measurements by Balog and co-workers that emphasized the use of extensively oxidized CaM, our results assayed the effect of modest amounts of methionine oxidation that mimic that observed in vivo where differences in the sensitivities of the CaM-dependent activation and inhibition of RyR1 to the oxidation of methionines in CaM are readily apparent (Figure 3). These latter results clearly resolve large differences in the CaM-dependent regulation of RyR1 channel activation (at nanomolar calcium levels) and channel inhibition (at micromolar calcium levels) and indicate the importance of investigating the functional effects of levels of methionine oxidation on RyR1 function that mimic that observed for CaM isolated in vivo.

Further, while our results emphasize the functional effects associated with the oxidation of methionines in CaM, prior measurements by Balog and co-workers emphasized CaM mutants involving the site-specific substitution of individual Mets with Gln, which do not "significantly disturb the structure of CaM because both amino acids have a similar propensity to form α-helices" (*9*). However, while this strategy has been used previously to effectively map how the binding of individual methionines in CaM contributes to the activation of target proteins (*68*−*71*), these mutants do not simulate the effects of methionine sulfoxide formation on CaM structure, as methionine sulfoxide does not pack well into helices and results in substantial changes in the structure of CaM (*1*, *37*, *42*, *45*). Indeed, it has been previously demonstrated that CaM mutants involving Met → Gln substitutions do not simulate the functional effects of methionine oxidation on the CaM-dependent activation of the plasma membrane Ca-ATPase (*48*, *70*). Thus, our data indicate that under conditions that promote the selective oxidation of methionines to their methionine sulfoxides, the calcium-activated form of oxidized CaM binds in a nonproductive conformation to RyR1 to disrupt the normal inhibition of channel function observed at micromolar calcium concentrations.

Regulation of RyR1 by CaM Oxidation. The observed functional modulation of RyR1 channel activity in response to the oxidation of CaM may act to prolong the duration of calcium transients and the associated generation of contractile force under conditions of oxidative stress. Indeed, alterations in the CaM-dependent regulation of RyR1 may be part of an adaptive mechanism that overcomes declines in the force of contraction that result from the sensitivity of the contractile filaments to oxidative stress (*62*, *63*). The mechanism of regulation involves the nonproductive association between the calcium-activated state of oxidized CaM and RyR1, which results in the disruption of structural transitions that normally enhance channel inhibition. In this respect, our prior measurements have demonstrated a correspondence between the calcium-dependent activation of the C- and N-domains of CaM and the associated CaM-dependent activation or inhibition of RyR1 function (*56*). At low nanomolar calcium levels associated with resting muscle, the C-terminal globular domain of CaM, with calcium sites III and IV occupied, is tethered to the high-affinity CaM-binding sequence RyRp (i.e., K^{3614}−N^{3643}) of RyR1 (Figure 9A). At these resting calcium levels, the N-domain of CaM is not associated with the CaM-binding sequence K^{3614}−N^{3643} in RyR1 but may bind to a noncontiguous binding site, such as the proposed N-terminal binding sequence of Ser^{1975}−Arg^{1999} on an adjacent subunit of RyR1 so that adjacent subunits of the channel are structurally coupled (*28*). A similar type of regulation by CaM has been proposed for the Cav1.2 calcium channel (*72*). Micromolar calcium concentrations promote occupancy of calcium-binding sites I and II to induce the structural collapse of the N-domain of CaM binding around the high-affinity sequence K^{3614}−N^{3643}, which is apparent in the high-resolution structure of the complex (*51*). Release of RyR1 intersubunit contact interactions mediated through CaM is suggested to promote the conformational relaxation of the RyR tetrameric complex necessary for channel closure (Figure 9B). Our current measurements demonstrate that oxidation of CaM disrupts the association between the opposing domains of calcium-activated CaM bound to RyRp that is required for normal channel closure (Figure 8) and therefore uncouples the normal calcium-dependent activation of CaM from RyR1 channel inhibition. The functional sensitivity of the CaM-dependent inhibition of channel activity, where the oxidation of approximately two methionines results in a 50% loss of functional regulation, suggests that the disruption of the normal binding of the N-terminal domain of CaM to the high-affinity CaM-binding sequence of the RyR tetrameric complex may be sufficient to maintain intersubunit interactions to effectively lock the channel in an activated state (Figure 9). Depending on cellular redox conditions, and relative rates of generation of reactive oxygen species and repair activities involving methionine sulfoxide reductase, the RyR1 open channel probability can rapidly respond to changes in cellular conditions through the reversible oxidation of CaM.

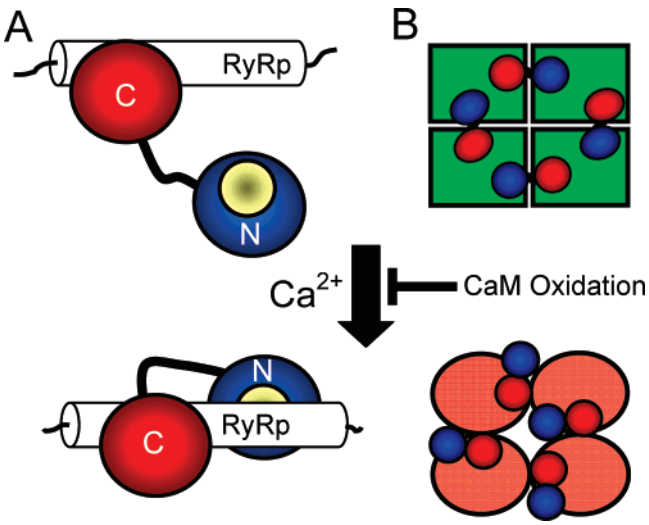

FIGURE 9: Met oxidation in CaM blocks calcium-dependent inhibition of RyR. Model depicting known binding interactions between N- and C-terminal domains of CaM, depicted in blue and red, between apo-CaM and calcium-activated CaM and the CaM-binding sequence RyRp in RyR1 (A) and oxidation-dependent inhibition of allosteric switching mechanism that promotes the transition between open (green) and closed (red) states of RyR1 (B). The binding cleft in calcium-activated CaM is colored yellow.

Conclusions and Future Directions. Multiple methionines in CaM are oxidized to their corresponding methionine sulfoxides in skeletal muscle, resulting in a nonproductive binding interaction with RyR1 and the selective inhibition of the normal CaM-dependent inhibition of channel activity observed at micromolar calcium levels. The ability to differentially modulate the CaM-dependent regulation of RyR1 channel activity at nanomolar and micromolar calcium levels associated with resting and activated muscles suggests an important physiological mechanism for rapidly modulating cytosolic calcium levels in response to cellular redox conditions. Moreover, the skeletal muscle ryanodine receptor, itself, exhibits inherent redox sensitivities that affect its gating properties through both cysteine oxidation and nitrosation (*73*, *74*). While this study has considered only the effects of CaM oxidation, RyR1 oxidation products should also be considered in future studies to build a complete functional picture of RyR1 under various redox conditions in contracting muscle.

ACKNOWLEDGMENT

We thank Dr. Todd Williams, Director of the Mass Spectometry Facility at the University of Kansas (Lawrence, KS), for mass spectrometry measurements of the distribution of CaM oxiforms.

REFERENCES

1. Bigelow, D. J., and Squier, T. C. (2005) Redox modulation of cellular signaling and metabolism through reversible oxidation of methionine sensors in calcium regulatory proteins, *Biochim. Biophys. Acta 1703*, 121−134.
2. Gao, J., Yin, D., Yao, Y., Williams, T. D., and Squier, T. C. (1998) Progressive decline in the ability of calmodulin isolated from aged brain to activate the plasma membrane Ca-ATPase, *Biochemistry 37*, 9536−9548.
3. Toda, T., Morimasa, T., Kobayashi, S., Nomura, K., Hatozaki, T., and Hirota, M. (2003) A proteomic approach to determination of the significance of protein oxidation in the ageing of mouse hippocampus, *Appl. Genomics Proteomics 2*, 43−50.
4. Ruse, C. I., Tan, F. L., Kinter, M., and Bond, M. (2004) Intregrated analysis of the human cardiac transcriptome, proteome and phosphoproteome, *Proteomics 4*, 1505−1516.
5. Li, J., Bigelow, D. J., and Squier, T. C. (2003) Phosphorylation by cAMP-dependent protein kinase modulates the structural coupling between the transmembrane and cytosolic domains of phospholamban, *Biochemistry 42*, 10674−10682.
6. Li, J., Bigelow, D. J., and Squier, T. C. (2004) Conformational changes within the cytosolic portion of phospholamban upon release of Ca-ATPase inhibition, *Biochemistry 43*, 3870−3879.
7. Li, J., Boschek, C. B., Xiong, Y., Sacksteder, C. A., Squier, T. C., and Bigelow, D. J. (2005) Essential role for Pro21 in phospholamban for optimal inhibition of the Ca-ATPase, *Biochemistry 44*, 16181−16191.
8. Bartlett, R. K., Bieber Urbauer, R. J., Anbanandam, A., Smallwood, H. S., Urbauer, J. L., and Squier, T. C. (2003) Oxidation of Met144 and Met145 in calmodulin blocks calmodulin dependent activation of the plasma membrane Ca-ATPase, *Biochemistry 42*, 3231−3238.
9. Balog, E. M., Norton, L. E., Bloomquist, R. A., Cornea, R. L., Black, D. J., Louis, C. F., Thomas, D. D., and Fruen, B. R. (2003) Calmodulin oxidation and methionine to glutamine substitutions reveal methionine residues critical for functional interaction with ryanodine receptor-1, *J. Biol. Chem. 278*, 15615−15621.
10. Balog, E. M., Norton, L. E., Thomas, D. D., and Fruen, B. R. (2006) Role of calmodulin methionine residues in mediating productive association with cardiac ryanodine receptors, *Am. J. Physiol. 290*, H794−H799.
11. Yang, H. C., Reedy, M. M., Burke, C. L., and Strasburg, G. M. (1994) Calmodulin interaction with the skeletal muscle sarcoplasmic reticulum calcium channel protein, *Biochemistry 33*, 518−525.
12. Tripathy, A., Xu, L., Mann, G., and Meissner, G. (1995) Calmodulin activation and inhibition of skeletal muscle Ca^{2+} release channel (ryanodine receptor), *Biophys. J. 69*, 106−119.
13. Rodney, G. G., Williams, B. Y., Strasburg, G. M., Beckingham, K., and Hamilton, S. L. (2000) Regulation of RYR1 activity by Ca^{2+} and calmodulin, *Biochemistry 39*, 7807−7812.
14. Moore, C. P., Rodney, G., Zhang, J. Z., Santacruz-Toloza, L., Strasburg, G., and Hamilton, S. L. (1999) Apocalmodulin and Ca^{2+} calmodulin bind to the same region on the skeletal muscle Ca^{2+} release channel, *Biochemistry 38*, 8532−8537.
15. Wagenknecht, T., Radermacher, M., Grassucci, R., Berkowitz, J., Xin, H. B., and Fleischer, S. (1997) Locations of calmodulin and FK506-binding protein on the three-dimensional architecture of the skeletal muscle ryanodine receptor, *J. Biol. Chem. 272*, 32463−32471.
16. Meissner, G. (1986) Evidence of a role for calmodulin in the regulation of calcium release from skeletal muscle sarcoplasmic reticulum, *Biochemistry 25*, 244−251.
17. Fuentes, O., Valdivia, C., Vaughan, D., Coronado, R., and Valdivia, H. H. (1994) Calcium-dependent block of ryanodine receptor channel of swine skeletal muscle by direct binding of calmodulin, *Cell Calcium 15*, 305−316.
18. Fruen, B. R., Bardy, J. M., Byrem, T. M., Strasburg, G. M., and Louis, C. F. (2000) Differential Ca^{2+} sensitivity of skeletal and cardiac muscle ryanodine receptors in the presence of calmodulin, *Am. J. Physiol. 279*, C724−C733.
19. Alseikhan, B. A., DeMaria, C. D., Colecraft, H. M., and Yue, D. T. (2002) Engineered calmodulins reveal the unexpected eminence of Ca^{2+} channel inactivation in controlling heart excitation, *Proc. Natl. Acad. Sci. U.S.A. 99*, 17185−17190.
20. Samso, M., and Wagenknecht, T. (2002) Apocalmodulin and Ca^{2+}-calmodulin bind to neighboring locations on the ryanodine receptor, *J. Biol. Chem. 277*, 1349−1353.
21. Taylor, C. W., and Laude, A. J. (2002) IP3 receptors and their regulation by calmodulin and cytosolic Ca^{2+}, *Cell Calcium 32*, 321−334.
22. Peterson, B. Z., DeMaria, C. D., Adelman, J. P., and Yue, D. T. (1999) Calmodulin is the Ca^{2+} sensor for Ca^{2+}-dependent inactivation of L-type calcium channels, *Neuron 22*, 549−558.
23. Xia, X. M., Fakler, B., Rivard, A., Wayman, G., Johnson-Pais, T., Keen, J. E., Ishii, T., Hirschberg, B., Bond, C. T., Lutsenko, S., Maylie, J., and Adelman, J. P. (1998) Mechanism of calcium gating in small-conductance calcium-activated potassium channels, *Nature 395*, 503−507.
24. Zuhlke, R. D., Pitt, G. S., Deisseroth, K., Tsien, R. W., and Reuter, H. (1999) Calmodulin supports both inactivation and facilitation of L-type calcium channels, *Nature 399*, 159−162.
25. DeMaria, C. D., Soong, T. W., Alseikhan, B. A., Alvania, R. S., and Yue, D. T. (2001) Calmodulin bifurcates the local Ca^{2}+ signal that modulates P/Q-type Ca^{2+} channels, *Nature 411*, 484−489.
26. Singh, B. B., Liu, X., Tang, J., Zhu, M. X., and Ambudkar, I. S. (2002) Calmodulin regulates Ca^{2+}-dependent feedback inhibition of store-operated Ca^{2+} influx by interaction with a site in the C terminus of TrpC1, *Mol. Cell 9*, 739−750.
27. Yamaguchi, N., Xin, C., and Meissner, G. (2001) Identification of apocalmodulin and Ca^{2+}-calmodulin regulatory domain in skeletal muscle Ca^{2+} release channel, ryanodine receptor, *J. Biol. Chem. 276*, 22579−22585.
28. Zhang, H., Zhang, J. Z., Danila, C. I., and Hamilton, S. L. (2003) A noncontiguous, intersubunit binding site for calmodulin on the skeletal muscle Ca^{2+} release channel, *J. Biol. Chem. 278*, 8348−8355.
29. Yin, D., Sun, H., Ferrington, D. A., and Squier, T. C. (2000) Closer proximity between opposing domains of vertebrate calmodulin following deletion of Met(145)-Lys(148), *Biochemistry 39*, 10255−10268.
30. Strasburg, G. M., Hogan, M., Birmachu, W., Thomas, D. D., and Louis, C. F. (1988) Site-specific derivatives of wheat germ calmodulin. Interactions with troponin and sarcoplasmic reticulum, *J. Biol. Chem. 263*, 542−548.
31. Yin, D., Kuczera, K., and Squier, T. C. (2000) The sensitivity of carboxyl-terminal methionines in calmodulin isoforms to oxidation by H_2O_2 modulates the ability to activate the plasma membrane Ca-ATPase, *Chem. Res. Toxicol. 13*, 103−110.
32. Mickelson, J. R., Ross, J. A., Reed, B. K., and Louis, C. F. (1986) Enhanced Ca^{2+}-induced calcium release by isolated sarcoplasmic reticulum vesicles from malignant hyperthermia susceptible pig muscle, *Biochim. Biophys. Acta 862*, 318−328.
33. Zhang, J. Z., Wu, Y., Williams, B. Y., Rodney, G., Mandel, F., Strasburg, G. M., and Hamilton, S. L. (1999) Oxidation of the skeletal muscle Ca^{2+} release channel alters calmodulin binding, *Am. J. Physiol. 276*, C46−C53.
34. Boschek, C. B., Squier, T. C., and Bigelow, D. J. (2007) Disruption of interdomain interactions via partial calcium occupancy of calmodulin, *Biochemistry 46*, 4580−4588.
35. Patton, C., Thompson, S., and Epel, D. (2004) Some precautions in using chelators to buffer metals in biological solutions, *Cell Calcium 35*, 427−431.
36. Nelson, D. P., and Kiesow, L. A. (1972) Enthalpy of decomposition of hydrogen peroxide by catalase at 25 °C (with molar extinction coefficients of H_2O_2 solutions in the UV), *Anal. Biochem. 49*, 474−478.
37. Gao, J., Yin, D. H., Yao, Y., Sun, H., Qin, Z., Schoneich, C., Williams, T. D., and Squier, T. C. (1998) Loss of conformational stability in calmodulin upon methionine oxidation, *Biophys. J. 74*, 1115−1134.
38. Xiong, Y., Chen, B., Smallwood, H. S., Urbauer, R. J., Markille, L. M., Galeva, N., Williams, T. D., and Squier, T. C. (2006) High-affinity and cooperative binding of oxidized calmodulin by methionine sulfoxide reductase, *Biochemistry 45*, 14642−14654.
39. Haugland, R. P. (2002) *Handbook of Fluorescent Probes and Research Products*, Molecular Probes, Inc., Eugene, OR.

40. Ledbetter, M. W., Preiner, J. K., Louis, C. F., and Mickelson, J. R. (1994) Tissue distribution of ryanodine receptor isoforms and alleles determined by reverse transcription polymerase chain reaction, *J. Biol. Chem. 269*, 31544−31551.
41. Lakowicz, J. R. (1999) *Principles of Fluorescence Spectroscopy*, 2nd ed., Kluwer Academic/Plenum Publishers, New York.
42. Ferrington, D. A., Sun, H., Murray, K. K., Costa, J., Williams, T. D., Bigelow, D. J., and Squier, T. C. (2001) Selective degradation of oxidized calmodulin by the 20 S proteasome, *J. Biol. Chem. 276*, 937−943.
43. Smallwood, H. S., Galeva, N. A., Bartlett, R. K., Urbauer, R. J., Williams, T. D., Urbauer, J. L., and Squier, T. C. (2003) Selective nitration of Tyr99 in calmodulin as a marker of cellular conditions of oxidative stress, *Chem. Res. Toxicol. 16*, 95−102.
44. Stadtman, E. R., Van Remmen, H., Richardson, A., Wehr, N. B., and Levine, R. L. (2005) Methionine oxidation and aging, *Biochim. Biophys. Acta 1703*, 135−140.
45. Sacksteder, C. A., Whittier, J. E., Xiong, Y., Li, J., Galeva, N. A., Jacoby, M. E., Purvine, S. O., Williams, T. D., Rechsteiner, M. C., Bigelow, D. J., and Squier, T. C. (2006) Tertiary structural rearrangements upon oxidation of methionine145 in calmodulin promotes targeted proteasomal degradation, *Biophys. J. 91*, 1480−1493.
46. Pessah, I. N., Waterhouse, A. L., and Casida, J. E. (1985) The calcium-ryanodine receptor complex of skeletal and cardiac muscle, *Biochem. Biophys. Res. Commun. 128*, 449−456.
47. Laver, D. R., Owen, V. J., Junankar, P. R., Taske, N. L., Dulhunty, A. F., and Lamb, G. D. (1997) Reduced inhibitory effect of Mg^{2+} on ryanodine receptor-Ca^{2+} release channels in malignant hyperthermia, *Biophys. J. 73*, 1913−1924.
48. Squier, T. C., and Bigelow, D. J. (2000) Protein oxidation and age-dependent alterations in calcium homeostasis, *Front. Biosci. 5*, D504−D526.
49. O'Connell, K. M., Yamaguchi, N., Meissner, G., and Dirksen, R. T. (2002) Calmodulin binding to the 3614−3643 region of RyR1 is not essential for excitation-contraction coupling in skeletal myotubes, *J. Gen. Physiol. 120*, 337−347.
50. Xiong, H., Feng, X., Gao, L., Xu, L., Pasek, D. A., Seok, J. H., and Meissner, G. (1998) Identification of a two EF-hand Ca^{2+} binding domain in lobster skeletal muscle ryanodine receptor/Ca^{2+} release channel, *Biochemistry 37*, 4804−4814.
51. Maximciuc, A. A., Putkey, J. A., Shamoo, Y., and Mackenzie, K. R. (2006) Complex of calmodulin with a ryanodine receptor target reveals a novel, flexible binding mode, *Structure 14*, 1547−1556.
52. Tikunova, S. B., Black, D. J., Johnson, J. D., and Davis, J. P. (2001) Modifying Mg^{2+} binding and exchange with the N-terminal of calmodulin, *Biochemistry 40*, 3348−3353.
53. Yao, Y., and Squier, T. C. (1996) Variable conformation and dynamics of calmodulin complexed with peptides derived from the autoinhibitory domains of target proteins, *Biochemistry 35*, 6815−6827.
54. Yao, Y., Gao, J., and Squier, T. C. (1996) Dynamic structure of the calmodulin-binding domain of the plasma membrane Ca-ATPase in native erythrocyte ghost membranes, *Biochemistry 35*, 12015−12028.
55. Ikura, M., Barbato, G., Klee, C. B., and Bax, A. (1992) Solution structure of calmodulin and its complex with a myosin light chain kinase fragment, *Cell Calcium 13*, 391−400.
56. Boschek, C., Jones, T., Squier, T. C., and Bigelow, D. J. (2007) Calcium occupancy of N-terminal sites within calmodulin induces inhibition of RyR1 calcium release channel, *Biochemistry 46*, 10621−10628.
57. Lehrer, S. S. (1997) Intramolecular pyrene excimer fluorescence: A probe of proximity and protein conformational change, *Methods Enzymol. 278*, 286−295.
58. Chen, B., Mayer, M. U., and Squier, T. C. (2005) Structural uncoupling between opposing domains of oxidized calmodulin underlies the enhanced binding affinity and inhibition of the plasma membrane Ca-ATPase, *Biochemistry 44*, 4737−4747.
59. Ehrhardt, M. R., Urbauer, J. L., and Wand, A. J. (1995) The energetics and dynamics of molecular recognition by calmodulin, *Biochemistry 34*, 2731−2738.
60. Slaughter, B. D., Urbauer, R. J., Urbauer, J. L., and Johnson, C. K. (2007) Mechanism of calmodulin recognition of the binding domain of isoform 1b of the plasma membrane Ca^{2+}-ATPase: Kinetic pathway and effects of methionine oxidation, *Biochemistry 46*, 4045−4054.
61. Crivici, A., and Ikura, M. (1995) Molecular and structural basis of target recognition by calmodulin, *Annu. Rev. Biophys. Biomol. Struct. 24*, 85−116.
62. Lowe, D. A., Surek, J. T., Thomas, D. D., and Thompson, L. V. (2001) Electron paramagnetic resonance reveals age-related myosin structural changes in rat skeletal muscle fibers, *Am. J. Physiol. 280*, C540−C547.
63. Thompson, L. V., Durand, D., Fugere, N. A., and Ferrington, D. A. (2006) Myosin and actin expression and oxidation in aging muscle, *J. Appl. Phys. 101*, 1581−1587.
64. Robison, A. J., Winder, D. G., Colbran, R. J., and Bartlett, R. K. (2007) Oxidation of calmodulin alters activation and regulation of CaMKII, *Biochem. Biophys. Res. Commun. 356*, 97−101.
65. Yao, Y., Yin, D., Jas, G. S., Kuczer, K., Williams, T. D., Schoneich, C., and Squier, T. C. (1996) Oxidative modification of a carboxyl-terminal vicinal methionine in calmodulin by hydrogen peroxide inhibits calmodulin-dependent activation of the plasma membrane Ca-ATPase, *Biochemistry 35*, 2767−2787.
66. Montgomery, H. J., Bartlett, R., Perdicakis, B., Jervis, E., Squier, T. C., and Guillemette, J. G. (2003) Activation of constitutive nitric oxide synthases by oxidized calmodulin mutants, *Biochemistry 42*, 7759−7768.
67. Osborn, K. D., Bartlett, R. K., Mandal, A., Zaidi, A., Urbauer, R. J., Urbauer, J. L., Galeva, N., Williams, T. D., and Johnson, C. K. (2004) Single-molecule dynamics reveal an altered conformation for the autoinhibitory domain of plasma membrane Ca^{2+}-ATPase bound to oxidatively modified calmodulin, *Biochemistry 43*, 12937−12944.
68. Chin, D., and Means, A. R. (1996) Methionine to glutamine substitutions in the C-terminal domain of calmodulin impair the activation of three protein kinases, *J. Biol. Chem. 271*, 30465−30471.
69. Chin, D., Winkler, K. E., and Means, A. R. (1997) Characterization of substrate phosphorylation and use of calmodulin mutants to address implications from the enzyme crystal structure of calmodulin-dependent protein kinase I, *J. Biol. Chem. 272*, 31235−31240.
70. Yin, D., Sun, H., Weaver, R. F., and Squier, T. C. (1999) Nonessential role for methionines in the productive association between calmodulin and the plasma membrane Ca-ATPase, *Biochemistry 38*, 13654−13660.
71. Chin, D., Sloan, D. J., Quiocho, F. A., and Means, A. R. (1997) Functional consequences of truncating amino acid side chains located at a calmodulin-peptide interface, *J. Biol. Chem. 272*, 5510−5513.
72. Morad, M., and Soldatov, N. (2005) Calcium channel inactivation: Possible role in signal transduction and Ca^{2+} signaling, *Cell Calcium 38*, 223−231.
73. Stamler, J. S., and Meissner, G. (2001) Physiology of nitric oxide in skeletal muscle, *Physiol. Rev. 81*, 209−237.
74. Petrotchenko, E. V., Pasek, D., Elms, P., Dokholyan, N. V., Meissner, G., and Borchers, C. H. (2006) Combining fluorescence detection and mass spectrometric analysis for comprehensive and quantitative analysis of redox-sensitive cysteines in native membrane proteins, *Anal. Chem. 78*, 7959−7966.

BI701352W